Ceramics International **23** (1997) 329–336

PII: S0272-8842(96)00032-6
0272-8842/97 $17.00+0.00

The Microstructure Analysis of Cerium-Modified Barium Titanate Having Core–Shell Structured Grains

Y. Park[a] & H. G. Kim[b]

[a]Department of Advanced Materials Engineering, Korea Advanced Institute of Science and Technology, P.O. Box 150, Cheongryang, Seoul, Korea
[b]Department of Materials Science and Engineering, Korea Advanced Institute of Science and Technology, Kusong-dong, Yusong-gu, Taejon, Korea

(Received 24 September 1995; accepted 1 March 1996)

Abstract: The microstructure of chemical inhomogeneity having the core–shell structured grain of cerium-modified barium titanate was investigated using X-ray, TEM, dilatometer and DSC methods. Specific heat anomalies, thermal expansion anomalies and lattice parameter discontinuities were associated with the three ferroelectric transitions (T_c, T_1 and T_2) of the grain-core of $BaTiO_3$. The crystal symmetry of the chemically inhomogeneous grain was strongly dependent on the cerium concentration and temperature. In comparison to other physical quantities, the temperature dependence of the dielectric constant was easily influenced by stress. © 1997 Elsevier Science Limited and Techna S.r.l.

1 INTRODUCTION

The commercial multilayer ceramic capacitors (hereafter abbreviated as MLCC) are mainly manufactured from additives-modified barium titanate.[1] Pure barium titanate displays three dielectric anomalies associated with the ferroelectric transition temperatures (T_c, T_1 and T_2). Therefore, the MLCC formulations can be chemically modified to meet the required temperature dependence of the dielectric constant, which can originate both from stress[2–4] and from the presence of chemically inhomogeneous grain.[5–12] The chemically inhomogeneous grain consists of three parts: grain-core, concentration gradient region and grain-shell. Since *in situ* TEM study, it has been apparent that (1) the temperature dependence of the dielectric constant relates to the chemically inhomogeneous grain (so-called compositional inhomogeneity), (2) that domain pattern's change of the grain-core exhibits the three ferroelectric transitions of pure $BaTiO_3$[12] with respect to temperature, and (3) that grain-core and grain-shell were not different phases. Then the temperature dependence of the dielectric constant may take the Lichtenecker type average of the three regions: grain-core, grain-shell, and concentration gradient region.[13]

For the application of the electronic component of MLCC, the specifications — mechanical strength, long term reliability and DC bias characteristics — become more important. Actually, these specifications were analysed to be closely associated with the grain size refinement. In order to meet the required temperature characteristic and above specifications, the recent formulation researcher for high capacitance MLCC was interested in the rare earth metal oxide-modified barium titanate — CeO_2, Sm_2O_3, Dy_2O_3, Gd_2O_3 and Nd_2O_3.[14–16] In particular, cerium-modified barium titanate was applied to Y5V (EIA's specifications that demand the dielectric constant does not change by more than +22%, −82% from 25 °C value over the temperature range of −25 °C to +85 °C) and Z5U (EIA's specifications that demand the dielectric constant does not change by more than +22%, −56% from 25 °C value over the temperature range of +10 °C to +85 °C). Compared with other MLCC formulation for high

capacitance, cerium-modified barium titanate has three strong points: firstly, is its simple composition which has two or three components. Secondly, because Curie temperatures are easily controlled by the amount of cerium, this formulation was applied to the custom-made MLCC. Thirdly, it has an excellent sinterability, reproducibility and simple manufacturing process without calcination.

Additions of CeO_2:1.5TiO_2 to $BaTiO_3$ decrease the tetragonality (c/a ratio), grain size and lower the Curie temperature (T_c) by approximately 30 °C per mol%. Even a small addition of 0.005 mole CeO_2:1.5TiO_2 to $BaTiO_3$ reduced the average grain size from 25 μm to 1.25 μm.

When $BaTiO_3$ cools through the ferroelectric transition (T_c), it undergoes a phase transition from cubic to tetragonal. Accompanying this phase change is a volume expansion (≅1.0%) which can lead to the development of complex stress state. It has been suggested that the stress system of grain-core may consist of a uniform compression along the c-axis, tensile stress along two a-axes, or a combination of the two. Because this stress would suppress the spontaneous deformation of tetragonal unit cell, forcing it to become more cubic, the temperature dependence of the dielectric constant was depressed and the three transition temperatures (T_c, T_1 and T_2) were shifted.

The object of this study was to examine the microstructure of the chemically inhomogeneous grain of cerium-doped $BaTiO_3$ with respect to temperature.

2 EXPERIMENTAL PROCEDURES

2.1 Sample preparation

The commercial high purity $BaTiO_3$ (99.6%) powder of BaO/TiO_2 mole ratio 1.002 in the present study was obtained from Kyoritsu Co., and synthesized by a conventional solid-state reaction process. All the additives used were reagent grade purity. The compositions chosen in this study are shown in Table 1. The appropriate mixtures of the additives to $BaTiO_3$ were pre-milled, mixed with the $BaTiO_3$ powders, pressed into a disk form. In order to control the grain size, the specimens were sintered between 1280 °C and 1400 °C for 4–1000 h. All the sintered ceramics have a fired density higher than 5.5 g/cm^3. The average grain sizes of the specimens were obtained from scanning electron microscopy (SEM) by the linear intercept method. The sintering conditions and average grain sizes are described in Table 1.

2.2 Characterization

Sintered ceramics were crushed to an average particle size of 40 μm to achieve the optimal orientation for X-ray diffraction analysis. Powder X-ray diffractions were conducted using an X-ray diffractometer equipped with a temperature-controlled attachment (−150 °C to +150 °C). Diffraction angles were corrected by a standard silicon target. More than five diffraction patterns from 20° to 110° (CuK_α, 2θ) were corrected to calculate the lattice parameters by using a least-squares determination.

In situ transmission electron microscopy (TEM) was carried out with a cooling/heating holder (−150 °C to +150 °C). Specimen temperatures were controlled by liquid nitrogen and by heat holder. The TEM specimens were coated with carbon to prevent discharge during observation. Details of TEM work and energy dispersive X-ray spectroscopy (EDS) are described in another paper.[12] TEM works for the micrography were operated at 300 kV, whereas the convergent beam electron diffraction (CBED) for crystal symmetry and lattice parameters were carried out with an operating voltage of 80 kV.

The temperature dependence of the dielectric constant was measured over a temperature range of −150 °C to +150 °C using a LCR meter at 1 kHz and 1 Vrms. Specific heat capacities (C_p) for samples were measured over the temperature range from 0 °C to 150 °C, using a Staton thermal analyser with a differential scanning calorimetric (DSC) cell. Approximately 30 mg of samples were added to a Pt boat and heated at a rate of 5 °C/h.

The linear thermal expansion coefficient (α) of the specimens has been measured at temperatures

Table 1. Compositions and grain size distributions

Specimen	Composition (mol)	Average grain size (μm)	Standard deviation of grain size (μm)	Sintering condition
A ceramic	$BaTiO_3$	20.4	4.2	1400 °C/4 h
B ceramic	0.963$BaTiO_3$–0.022CeO_2–0.015TiO_2	3.0	2.2	1280 °C/10 min
C ceramic	0.963$BaTiO_3$–0.022CeO_2–0.015TiO_2	1.8	0.37	1280 °C/4 h
D ceramic	0.963$BaTiO_3$–0.022CeO_2–0.015TiO_2	1.7	0.37	1300 °C/50 h
E ceramic	0.963$BaTiO_3$–0.022CeO_2–0.015TiO_2	1.7	0.32	1320 °C/1000 h

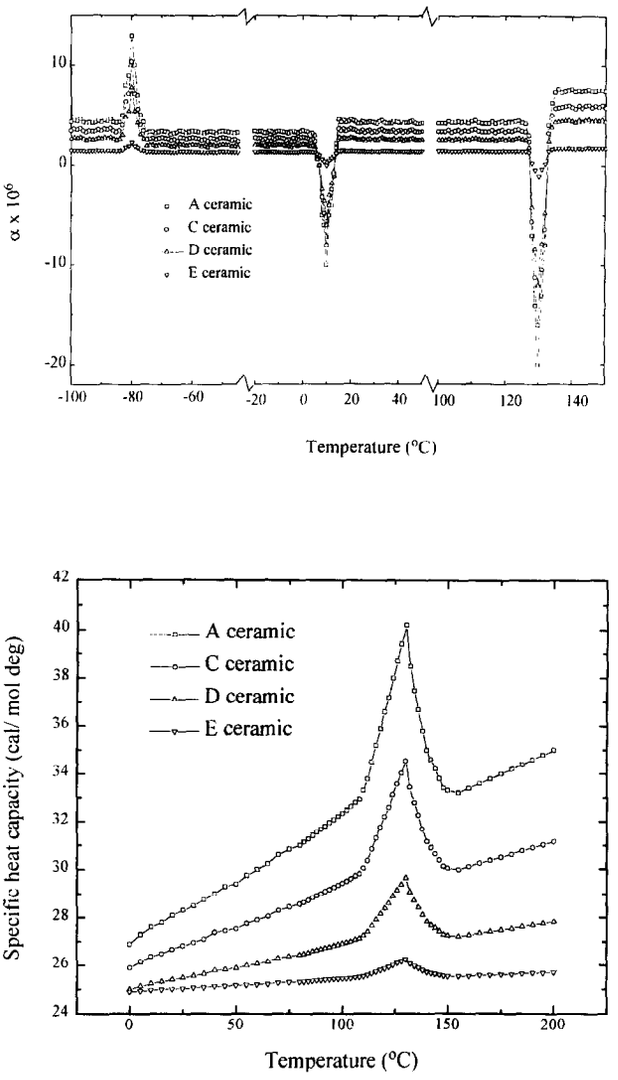

Fig. 1. (a) Thermal expansion coefficient (α), and (b) specific heat capacity of A, C, D and E ceramics as a function of temperature.

from −150 °C to +150 °C. The dilatometric test sample has a cylindrical form, 3 cm in length and 4 mm in diameter. Differential dilatation of the specimens relative to a silica rod was magnified by about 1000 times by means of an optical lever. The accuracy of thermal expansion coefficient is about 1×10^{-6}.

3 RESULTS

3.1 Thermal analysis

Figures 1(a) and (b) show the thermal expansion coefficient (α) and specific heat capacity (C_p) as a function of temperature, respectively. For A, C, D and E ceramics, the three peak temperatures of thermal expansion coefficient (α) at 130 °C, 10 °C and −80 °C were analysed to be associated with the three ferroelectric transition temperatures of T_c for cubic to tetragonal, T_1 for tetragonal to orthorhombic, and T_2 for orthorhombic to rhombohedral, respectively.

It is interesting that for C, D and E ceramics with different sintering conditions, the three peak intensities of thermal expansion coefficients (α) at temperatures associated with T_c, T_1 and T_2 were inversely proportional to the sintering times, which was attributable to the diffusion of cerium into the $BaTiO_3$ lattice. In contrast with the intensity, the three peak temperatures of α related to T_c, T_1 and T_2 were invariable regardless of the sintering conditions, which suggested that any lattice diffusion of additives into the grain-cores was not allowed.

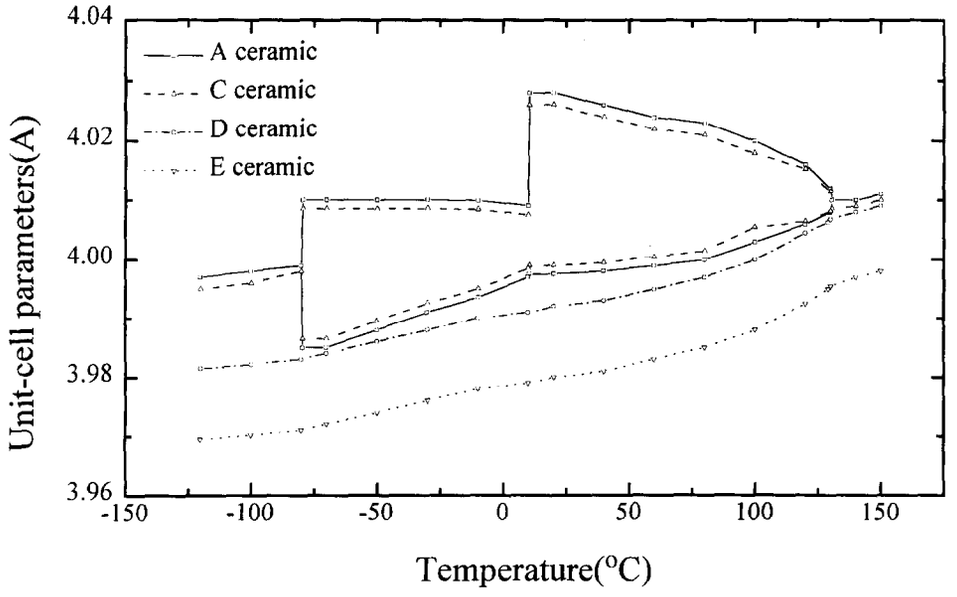

Fig. 2. Lattice parameters of A, C, D and E ceramics as a function of temperature.

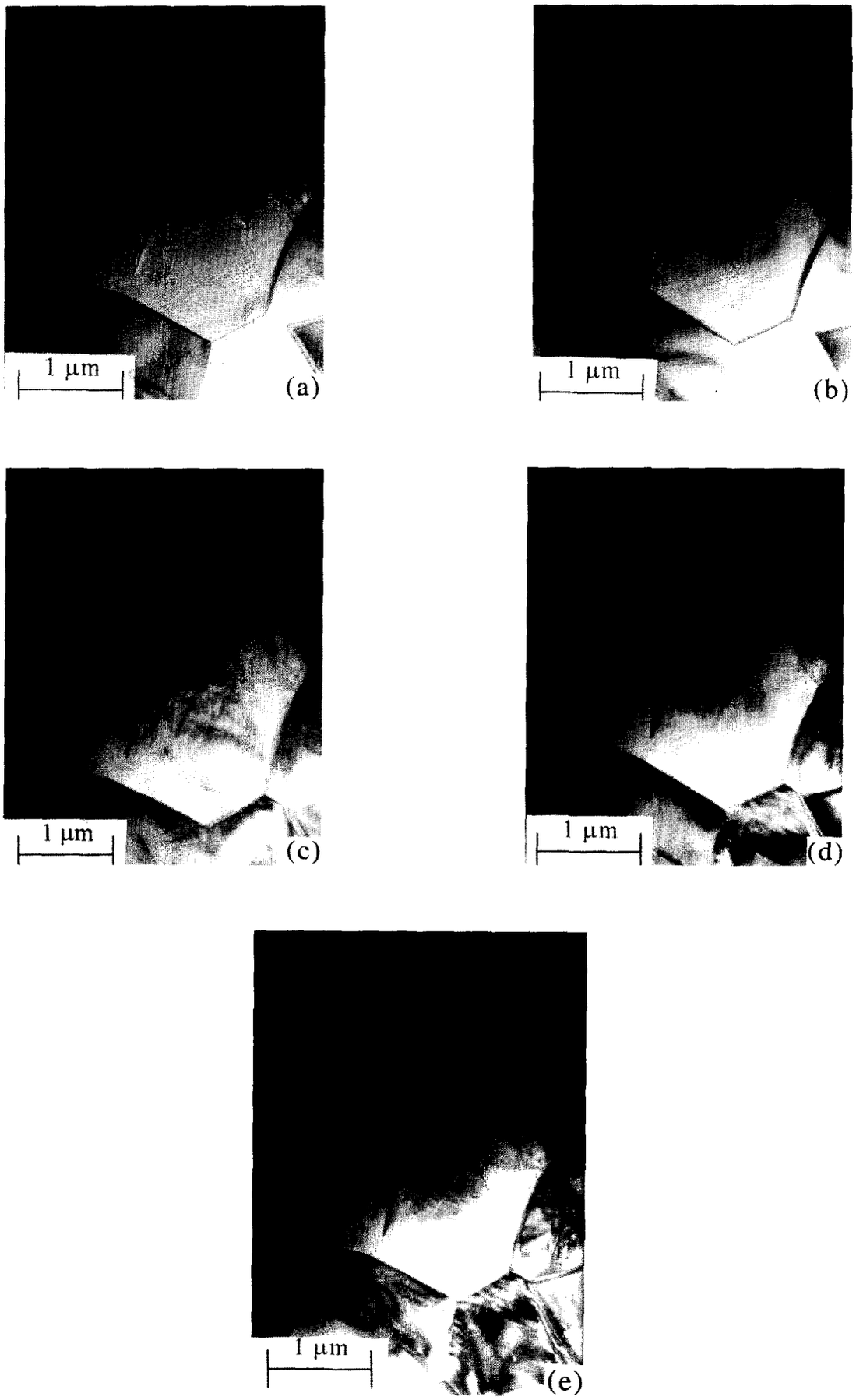

Fig. 3. TEM images of C ceramics at various temperatures: (a) 130 °C, (b) 25 °C, (c) −30 °C, (d) −70 °C and (e) −130 °C.

As shown in Fig. 1(b), the transition temperature and peak intensity of C_p at 130 °C are similar to those of α for A, C, D and E ceramics. Consequently, it was suggested that the three peak intensities of α and C_p associated with T_c, T_1 and T_2 may be strongly related to the volume fraction of grain-core of pure $BaTiO_3$, whereas three peak temperatures related to the purity of grain-core of $BaTiO_3$.

3.2 X-ray diffraction

The results for lattice parameters as a function of temperature are shown in Fig. 2. A and C ceramics exhibit the three discontinuities associated with three ferroelectric transition temperatures (T_c, T_1 and T_2) at 130 °C, 10 °C and −80 °C, respectively. In contrast to A ceramic of pure $BaTiO_3$, C ceramic of cerium-modified $BaTiO_3$ has small tetragonality (c/a ratio) and small unit cell dimensions, which is ascribed to the fact that Ce addition to $BaTiO_3$ stabilizes the cubic phase and that the Ce^{+4} replaces Ba^{+2} in $BaTiO_3$, to some extent. Therefore, it is suggested that with the increase of sintering time and sintering temperature, the volume fraction of grain-core of pure $BaTiO_3$ decreases. There are no discontinuities of lattice parameters at T_c, T_1 and T_2 for D and E ceramics, which was due mainly to the decrease of volume fraction of grain-core and stress caused by unit cell volume difference between grain-core and grain-shell.

Fig. 4. TEM image of C ceramic at 25 °C; even a small grain of 0.3 μm reveals the ferroelectric domain of grain-core.

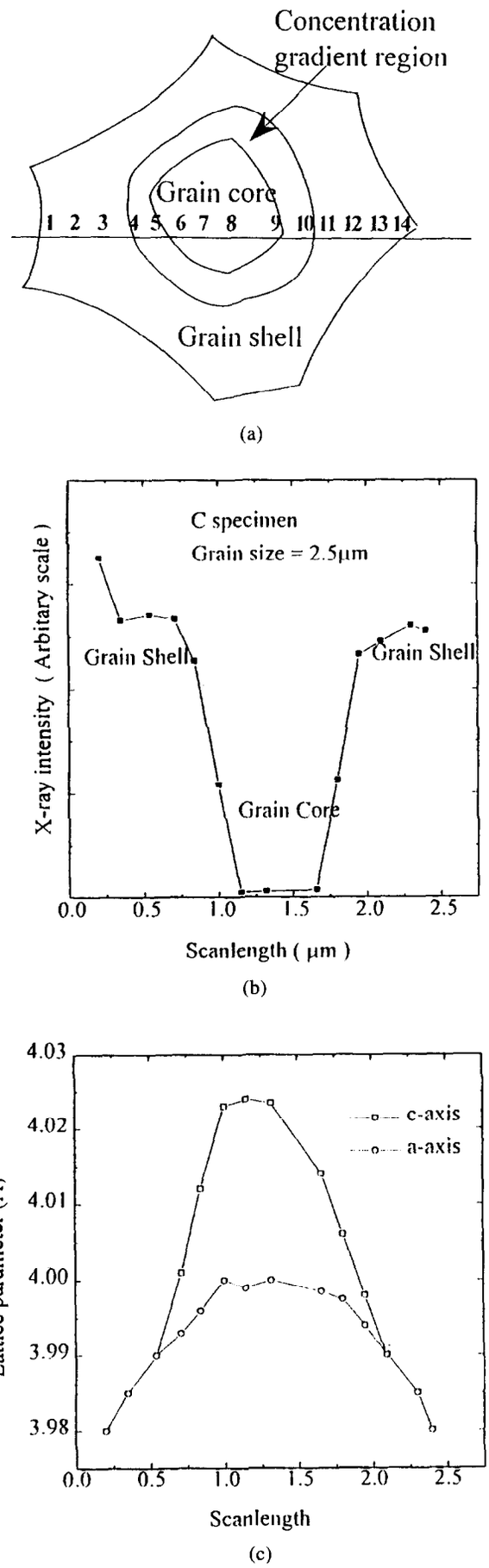

Fig. 5. STEM microanalysis for Ce in grain-core, concentration gradient region and grain-shell: (a) schematic diagram of core–shell structure based on the result of Fig. 3(b), (b) EDS analysis of Fig. 3(b), and (c) lattice parameters of Fig. 3(b).

3.3 TEM work

TEM micrographs of Fig. 3 (a), (b), (c), (d) and (e) for C ceramic were taken at 130 °C, 25 °C, −30 °C, 70 °C and −130 °C, respectively. Judging from the different domain patterns at various temperatures of TEM work, it was assumed that the grain-core at 130 °C, 25 °C, −30 °C, −70 °C and −130 °C belongs to the cubic, tetragonal, orthorhombic, rhombohedral and rhombohedral phases, respectively. Therefore, we came to the conclusion that the grain-core of pure $BaTiO_3$ undergoes three ferroelectric transitions of T_c, T_1 and T_2. With decreasing TEM work temperature, domain patterns become finer. Thus it is difficult to observe the domain of the grain-core at −130 °C.

Figure 4 shows the TEM image of C ceramic at room temperature. It is surprising that even a small grain with a grain size of 0.3 μm reveals the ferroelectric domain of grain-core at room temperature. We can expect that the grain-core is under compressive stress, because of the volume difference of unit cell between grain-core and grain-shell. Although the compressive stress and the small grain size of 0.3 μm stabilize the paraelectric cubic phase, it is impossible for this stress to annihilate the ferroelectric domain of the tetragonal grain-core with the size of 0.1 μm.

Figure 5 (a), (b) and (c) represent the schematic diagram based on the result of Fig. 3(b), EDS analysis and lattice parameter variations, respectively. At room temperature, grain-core, concentration gradient region and grain-shell correspond to tetragonal, orthorhombic and pseudocubic structures, respectively. The tetragonality (c/a ratio) of the concentration gradient region was inversely proportional to the amount of cerium. Moreover, we can expect the so-called diffuse phase transition because the concentration gradient region was mainly suggestive of the chemically inhomogeneous grain and Curie temperature distributions.

Conversant beam electron diffraction (CBED) was used to determine the crystal symmetry and lattice parameter for the grain of Fig. 3(b). The lattice parameter and the crystal symmetry were analysed over the temperature range from +135 °C to −150 °C, respectively. The analysis was carried out with respect to the <100> beam direction. The crystal symmetry of grain-core, grain-shell and concentration gradient region based on the result of Fig. 5(a) are described in Table 2 with regard to TEM work temperatures.

The grain-core exhibits the crystal symmetry of pure $BaTiO_3$. Judging from the fact that the crystal symmetry of the concentration gradient region was influenced by cerium concentration, we know that, according to the addition of Ce to $BaTiO_3$, T_c was shifted to a lower temperature, and T_1 and T_2 shifted to a higher temperature. The effect of cerium addition to $BaTiO_3$ on three ferroelectric temperatures (T_c, T_1, and T_2) was in good agreement with previous results.[1,12] On the contrary, the grain-shell of $BaTiO_3$ severely doped with CeO_2 always belongs to the pseudocubic structure, regardless of the TEM work temperatures.

4 DISCUSSION

Figure 6 shows the temperature dependence of the dielectric constant for all specimens. A ceramics exhibit the three peaks of pure $BaTiO_3$ associated with T_c, T_1 and T_2, whereas B ceramics display the two peaks: the first sharp peak at 130 °C was due to the grain-core of pure $BaTiO_3$, and the second broad peak around 60 °C is due to the concentration gradient region and grain-shell. With increase of sintering time, the three transition peaks (T_c, T_1 and T_2) become closer, and finally merge into a single peak. The increase and broadening of dielectric peak intensity is attributable to an overlap of three ferroelectric transition peaks. Therefore, the temperature dependence of the dielectric constant of barium titanate based core–shell structured ceramics was assumed to be a superposition of dielectric constant of ferroelectric grain-cores, paraelectric grain-shells, and concentration gradient region. So we applied the logarithmic mixing rule of

$$\log k = V_{\text{core}} \log k_{\text{core}} + V_{\text{con}} \log k_{\text{con}} + V_{\text{shell}} \log k_{\text{shell}}$$

Table 2. Crystal symmetry with respect to the TEM work temperature

Temperature	Grain-core	Concentration gradient region	Grain-shell
135 °C	Cubic	Cubic	Pseudocubic
100 °C	Tetragonal	Cubic	Pseudocubic
70 °C	Tetragonal	Tetragonal	Pseudocubic
25 °C	Tetragonal	Orthorhombic	Psuedocubic
−30 °C	Orthorhombic	Orthorhombic	Pseudocubic
−50 °C	Orthorhombic	Rhombohedral	Pseudocubic
−80 °C	Rhombohedral	Rhombohedral	Pseudocubic
−130 °C	Rhombohedral	Rhombohedral	—

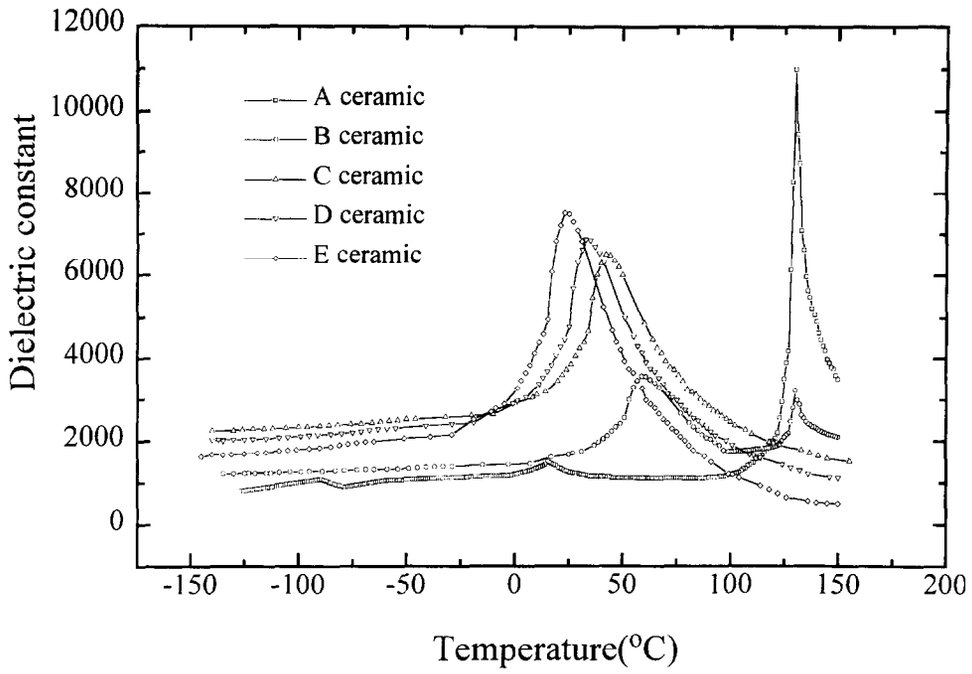

Fig. 6. Dielectric constant of A, B, C, D and E ceramics as a function of temperature.

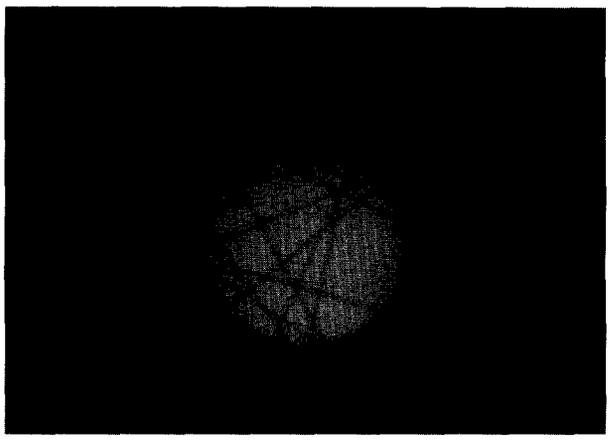

Fig. 7. Experimental HOLZ pattern taken in the [421] beam direction in the grain-core.

where V_{core}, V_{con}, and V_{shell} are the volume fraction of grain-core, concentration gradient region, and grain-shell, and where k_i is the dielectric constant of the region i.

Although there exists the ferroelectric domain of grain-core for C, D and E ceramics, we cannot observe the ferroelectric transition peak at 130 °C in Fig. 6. Analysis in the [421] beam direction was found to be sensitive to the strain in the lattice. Such a clear higher-order Laue zone (HOLZ) pattern in Fig. 7 is indicative of uniform strain across the grain-core region. Therefore, the reason why C, D and E ceramics do not exhibit the ferroelectric transition (T_c) at 130 °C was analysed to be associated (1) with the stress induced by grain size refinement and by the structural changes (i.e. formation of a pseudo-cubic perovskite), and (2) with small volume fraction of grain-core. Especially, in comparison to the other physical quantities (C_p, α and lattice parameters), the temperature dependence of the dielectric constant seems to be more sensitive to stress.

5 CONCLUSIONS

The chemically inhomogeneous grain of cerium-modified $BaTiO_3$ consists of three parts: grain-core, grain-shell, and concentration gradient region. The crystal symmetry and the lattice parameters of the chemically inhomogeneous grain were determined by cerium concentration and by temperature. The peak temperatures and peak intensities for C_p and α at temperatures associated with three ferroelectric transitions (T_c, T_1 and T_2) were dependent on the purity of the grain-core of $BaTiO_3$ and volume fraction of grain-core, respectively. Even a small grain with a grain size of 0.3 μm revealed the ferroelectric domain of the grain-core. In contrast with other physical quantities (α, C_p and lattice parameters), the temperature dependence of the dielectric constant was easily influenced by the stress.

REFERENCES

1. ZAFFE, B., COOK, W.R. & JAFFE, H., *Piezoelectronic Ceramics in Nonmetallic Solid: Series of Monographs No. 3*. Academic Press, London, 1971, p. 53.
2. YAMAJI, A., ENOMOTO, Y., KINOSHITA, K. & MURAKIMI, T., Preparation, characterization and properties of Dy-doped small grained $BaTiO_3$. *J. Am. Ceram. Soc.*, **60** (1977) 97–101.

3. MARKULICH, T. M., MAGDER, J., VUKASOVICH, M. S. & LOCKHART, R. J., Ferroelectric of ultrafine particle size: II. Grain growth inhibition studies. *J. Am. Ceram. Soc.*, **49** (1966) 295–299.
4. ALRT, G., HENNINGS, D. & DE WITH, G., Dielectric properties of pure barium titanate ceramic. *J. Appl. Phys.*, **58** (1985) 1619–1625.
5. RAWAL, B. S., KAHN, M. & BUESSEM, W. R., Grain core shell structure in barium titanate based dielectric. In *Advances in Ceramics*. American Ceramic Society, Columbus, OH, 1981, pp. 172–188.
6. ARMSTRONG, T. R. & BUCHANAN, R. C., Influence of core shell grains on the internal stress state and permittivity response of zirconia-modified barium titanate. *J. Am. Ceram. Soc.*, **73** (1990) 1268–1273.
7. LU, H. Y., BOW, J. S. & DENG, W. H., Core–shell structures in ZrO_2-modified $BaTiO_3$ ceramic. *J. Am. Ceram. Soc.*, **73** (1990) 3563–3568.
8. HENNINGS, D. & SCHNELL, A., Diffuse phase transition in $Ba(Ti_{1-y}Zr_y)O_3$. *J. Am. Ceram. Soc.*, **6** (1982) 539–544.
9. HENNING, D. & ROSENTEIN, G., Temperature-stable dielectric based chemically inhomogeneous $BaTiO_3$. *J. Am. Ceram. Soc.*, **67** (1984) 249–254.
10. KAHN, M., Influence of grain growth on dielectric properties of Nb-doped $BaTiO_3$. *J. Am. Ceram. Soc.*, **54** (1971) 455–457.
11. CHOI, C. J. & PARK, Y., The X7R phenomenon in the core–shell structured ceramics. *Ceram. Trans.*, **8** (1990) 148–156.
12. PARK, Y. & SONG, S. E., Influence of core–shell structured grain on dielectric properties of cerium-modified barium titanate. *J. Mater. Sci.: Mater. in Elec.*, **6** (1995) 380–388.
13. PARK, Y. & KIM, Y. H., The dielectric temperature characteristic of additives modified barium titanate. *J. Mater. Res.*, **10** (1995) 2770–2776.
14. PARK, Y., Unpublished paper.
15. PARK, Y., SONG, I. Y. & AHN, K. S., Korean Patent 90-13543, 1990.
16. PARK, Y. & KIM, C. I., Korean Patent 91-11699, 1991.